Thesis proposal

Task-oriented viewpoint planning for free-form non-rigid objects

Sergi Foix Salmerón

Director
Guillem Alenyà, Ph.D.(IRI)

Co-Director
Carme Torras, Ph.D.(IRI)

Doctorat en Automàtica, Robòtica i Visió

July 15, 2012

Contents

1 Introduction

In robotics, sensor viewpoint planning tries to exploit the process of modifying the pose of a sensor to acquire a new view of the scene. All tasks requiring multiple views (modelling, recognition, inspection, feature discovery...) can be interpreted as information gain processes, since an increment of information is expected with every new view. Although this information has been classically used for geometrical modelling under Next-Best-View (NBV) approaches, it should not be limited to them. Specially when dealing with unknown scenarios, the system should be able to decide new actions based only on the available information, the task-related goal and the expected reward of executing the selected next action. In such scenarios, the abilities to explicitly measure the gain of each action and to wisely choose a strong-related internal representation are crucial. A general and formal definition of active sensor planning, or also briefly known as active sensing, was stated by Bajcsy [6] in the late eighties as: "a problem of controlling strategies applied to the data acquisition process which will depend on the current state of the data interpretation and the goal or task of the process".

Active sensing systems are composed by three distinctive elements:, a vision system, a positioning system, and a view planner. The vision system, in our case a Time-of-Flight (ToF) 3D camera, is the one in charge of providing raw data from the environment. The positioning system, a 7 Degrees-of-Freedom (DoF) robotic manipulator in our case, is in charge of changing the camera's point of view according to the view planner's decision. Finally, the view planner is the core of the active sensing approach, the one that processes the incoming data and decides where the camera must be placed, and which must be its parametrization to succesfully achieve the goal of the task. Figure 1 shows two different examples of active sensing setups.

(a) 3D object modelling setup (b) Plant monitoring setup

Figure 1: Examples of two of the different active sensing setups used during this research. (a) High precision Kuka KR16 manipulator with a SR4000 ToF camera. (b) WAM manipulator with PMD CamBoard ToF camera and chlorophyll meter tool.

Active sensing tasks can be classified depending on different criteria, such as, the type of sensor used, the type of data representation, the goal of their tasks, or as it has been commonly categorized, depending on their previous knowledge of the scene. Based on the latter, tasks are divided as: model-based, non-model-based and partial-model-based. The classification is quite straightforward, model-based tasks are those that need an a priori complete knowledge of the object of interest, while non-model-based tasks are those who do not need it or they just can not have it. And finally, partial-model-based tasks are those that can only be optimally fulfilled if elemental task-oriented guidance is provided. Figure 2 shows the different active sensing tasks based on this structure.

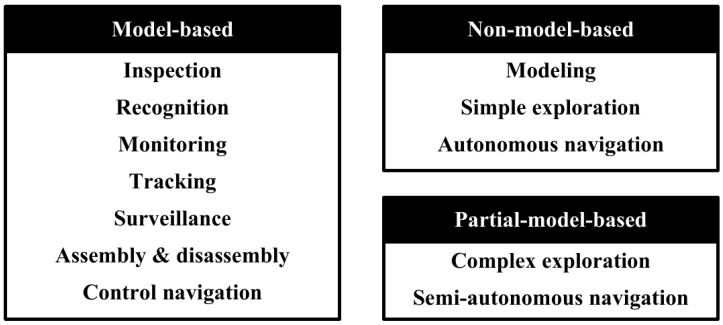

Figure 2: Classification of active sensing tasks depending on the knowledge of the scene.

Multiple requirements must be considered before the development of an active sensing system. Scott *et al.* [50] presented on their survey a set of requirements with the purpose of evaluating and posteriorly comparing the different object reconstruction planning algorithms. The bigger the number of requirements satisfied by the system, the higher the robustness and reliability.

It is important to mention here that at the time of the defense of this thesis proposal, a large part of the research has already been accomplished and, consequently, its results published. When required, the corresponding work will be properly introduced and referenced.

Category	Requirement	Maver & Bajscy [38]	Connolly [13]	Yuan [59]	Banta et al. [7]	Massios & Fisher [37]	Tarbox & Gottschlich [53]	Reed et al. [44]	Whaite & Ferrie [57]	Pito [43]	Papadopoulos-Orfanos [42]	PhD candidate
General	Model quality specification	N	N	N	N	N	N	N	N	N	N	N
	Generalizable algorithm	N	Y	N	Y	Y	Y	Y	N	Y	N	Y
	Generalized viewpoints	N	N	N	N	N	N	N	N	N	N	Y
	View overlap	N	N	N	N	N	N	N	P	P	N	Y
	Robust	N	N	N	N	?	?	?	N	?	?	Y
	Efficient	N	?	?	?	?	N	?	N	?	N	N
	Self-terminating	N	Y	Y	Y	Y	Y	Y	Y	Y	Y	Y
Object	Minimal a priori knowledge	Y	Y	Y	Y	Y	-	Y	N	Y	Y	Y
	Shape constraints	N	Y	N	Y	Y	Y	Y	N	Y	Y	Y
	Material constraints	N	N	N	N	N	N	N	N	N	N	Y
Sensor	Frustrum modeled	N	N	N	N	N	N	P	N	P	Y	Y
	Shadow effect	Y	N	N	N	N	Y	N	N	Y	Y	-
	Measurement performance	N	N	N	N	P	P	N	P	P	N	Y
Positioning System	6D pose	N	N	N	N	N	N	N	N	N	Y	Y
	Pose constraints	N	N	N	N	Y	Y	Y	N	Y	Y	Y
	Positioning performance	N	N	N	N	N	P	N	N	N	N	P

Table 1: Comparison of reconstruction planning algorithms [7, 13, 37, 38, 42, 43, 44, 53, 57, 59]. Where [Y] means requirement satisfied, [N] not satisfied, [P] partially satisfied, [?] uncertain and [-] not applicable.

2 Objectives and scope

2.1 Objectives

The main goal of the proposed thesis is to develop new vantage point decision-making algorithms for 3D-sensor-based real exploratory tasks over partially modelled free-form complex scenes under an information-gain paradigm. Therefore, this thesis will study new ways to generate goal-driven vantage points for complex task solving further than the classical 3D modelling task. Nevertheless, a previous deep study of the classical 3D object modelling task, commonly known as NBV planning, will be necessary to strongly establish the basis of the new approach.

To successfully complete the overall research the following tasks should be fulfilled:

1. **Characterize ToF camera uncertainty and constraints**. To efficiently accomplish the goal in a real robotic task, with real sensors and actuators, entails to efficiently deal with perception and action uncertainties. Therefore the main objective in this task is to define a methodology to calibrate and characterize ToF camera measurements.

2. **Improve data registration by profiting from sensor characterization**. High level task fulfillment require a correct understanding of high level perception entities. The 3D modelling task, as simple as multiple point clouds registration, is viewed as the lowest level task for exploration purposes.

3. **Define an information-gain approach as a task-based criterion for active sensing**. Exploring the world is nothing but to gain knowledge of it by gathering new data. Therefore it seems adequate to use an information-gain goal-driven approach as the basis for exploration tasks.

4. **Validate the approach by applying it to classical 3D modelling for free-form rigid objects**. By representing the unexplored scene as a voxelized 3D space, 3D object modelling can be seen as the task of prunning empty volumes and tagging occupied ones. An information-gain approach seems ideal for optimally searching the space, not re-visiting already seen views and allowing self-termination.

5. **Study the extraction of higher level 3D entities (visual/3D features) for the purposes of determining those that synthesize a specific task-oriented goal**. Once the complexity of the task increases, raw data by its own is not helpful anymore and higher level 3D entities must be determined in order to achieve the task's goal.

6. **Validate the approach by extending it to task-oriented active sensing of complex objects**. We will concentrate on plants: they are free-form, difficult to characterize and change over time. Examples of such complex tasks are: finding the area of a leaf, counting the number of leaves, or finding the best probing point for chlorophyll measurement.

2.2 Scope

As it has been presented in the previous section, the scope of this thesis goes beyond simple 3D NBV modelling and tries to extend 3D active sensing current methodology by including the goal of exploratory tasks into the decision-making process. Active sensing is too wide for covering all its topics, so to adequately complete the proposed research, the PhD thesis scope will focus on:

1. 3D ToF cameras, and RGB camera when needed, as vision system. The methodology can be easily adapted to other technologies. For instance, the use of RGB-D cameras, such

as Kinect. However, this type of cameras are not suitable for this research, due to their limitation in close depth range and its incapability to measure in outdoor settings under the presence of sunlight.

2. Robotic manipulator as positioning system. This way the camera can be placed at any pose in space. The only constraint is the robot's working space. Since our aim is monitoring medium sized plants, this constraint is not a big drawback. If a wider working space would be needed, the possibility of adding a revolving plate would be considered.

3. Information-gain as a general decision-making approach for task-oriented active sensing.

3 Previous Work

3.1 ToF Cameras

ToF cameras are a relatively new type of sensor that deliver 3-dimensional imaging at a high frame rate, simultaneously providing intensity data and range information for every pixel (see the current commercial ToF cameras in Fig. 3). Despite the number of pixels in the images is still small (i.e 176×144 in Swissranger SR3000 and SR4000 cameras, and 204×204 in PMD CamCube camera) and noise in the depth values can not yet be completely removed after calibration, ToF imaging has rapidly shown a great potential in numerous scientific domains. During the last 2 decades multiple contributions have appeared on diverse fields, such as robot navigation, obstacle avoidance, human-machine interfaces, or object modelling among others.

(a) SR4000, 176x144 (b) O3D100, 64x48 (c) CamCube 2.0, 204x204 (d) CamBoard, 200x200

Figure 3: Current commercial lock-in ToF cameras. (a) Mesa Imaging AG© [2]. (b) Ifm electronic© [1].(d-e) PMD[Vision]® [3]. Particularities of each solution include the use by CanestaVision™ of square modulated waves [25], the use of a smart pixel - photonic mixer device (PMD) for simultaneous wave sensing and mixing by PMD[Vision]® [58], and the addition by Mesa Imaging AG© of a coded binary sequence (CBS) modulation for multi-camera operation on SR4000 new models.

A competing sensing technology for active sensing tasks is lidar scanning, due to its precision, but which requires mobile parts to aggregate linear readings into full 3D scans with the subsequent detriment in frame rate. Stereo vision systems have also been used for such purposes, but require objects to be textured. On the contrary, ToF cameras offer registered depth-intensity images at high frame rate. Additionally, they offer other technical advantages, such as robustness to illumination changes, low power consumption and low weight. RGB-D camera also provide such advantages but, as it has been commented before, are incapable of working under sun conditions and they are not built for close range applications. Deeper information about ToF cameras and their applications can be found in Foix *et al.* [20, 22]

3.2 Sensor view planning

Sensor view planning has been commonly used for the tasks of precise geometrical model construction and object recognition (see the reviews [45, 50]), and to a lesser extent for the optimal segmentation of particular object characteristics [36, 48] and to exploit sensor features to easily detect occlusions, formerly using a laser [38] and more recently with a ToF sensor by Foix *et al.* [19].

These algorithms can be classified according to the constraints they impose on the type of objects that can handle, the sensors they use, the restrictions of the sensor positioning system, and more important, the decision-making strategy and the symbolic object representation they used. In [49] objects are represented statistically by multidimensional receptive field histograms, and the camera is controlled by making hypotheses on the salient points of the previously learned objects and then moving to the most discriminative viewpoint. In [15] reinforcement learning is used to associate the current state with camera actions and their corresponding reward. Here the model is a particle representation, and it is updated with new sensor readings with the Condensation algorithm. Earlier, this mapping between camera actions and new information was coded using entropy maps [5] and information-gain optimizations [17]. Other approaches to viewpoint selection include probabilistic reasoning [46] and Bayesian networks [33]. More recently, a boost-based algorithm to combine different appearance estimators [27] has been proposed to compute the next view in a rotating object framework.

All the previous algorithms require some degree of training. When training is not applicable or too expensive, approaches using information-gain measures are a good alternative. In such approaches, two steps can be clearly distinguished: the generation of a set of viewpoint candidates and the ranking of such candidates by evaluating the expected information gain of each action. Again, for viewpoint generation, the internal representation of the environment model plays an important role. Surface-based methods provide a set of viewpoints based on the location of jump edges [39], the trend of a contour [34] or the fitting of a parametric surface representation [4]. Volumetric methods provide viewpoints using the information of visited and non-visited portions of the workspace, and generally encode this space using voxel representations (or, more efficiently, octrees).

Information gain has been used before as viewpoint selection criterion in classical object modelling works [14], where the sensor uncertainty is modelled using only the viewing direction and is considered uniform for all the acquired points. While some approaches require some degree of overlap to match consecutive sensor readings, other methods do not (see [10] for a review) and consider this to be a positive feature. This is true for precise sensors, and for precise positioning systems, but it is not so when considering noisy sensors, specially when sensor readings have different uncertainties depending on their position on the image, as it is here the case with ToF cameras.

4 Workplan & expected contributions

The following is a description of the complete research work planning divided by tasks and also, their expected contributions at their accomplishment. A substantial subset of the tasks has been already fulfilled and, consequently, a detailed description of their contributions will be given.

4.1 Task 0: Background research

The PhD candidate holds an Industrial Technical Engineering degree in Electronics (specialized in Automatic Control) from the Universitat Politècnica de Catalunya (UPC), a BEng(Honors)

Communication and Electronic Engineering degree from Northumbria University, a MSc(Merit) Intelligent Systems from Sunderland University and a MSc Automatic Control and Robotics from UPC. Some of the most relevant studied topics related to this thesis are:

- Vision and intelligent robots (MSc IS)
- Intelligent systems programming (MSc IS)
- Advanced computer vision (MSc ACR)
- Mobile robotics and navigation (MSc ACR)
- Planning in robotics (MSc ACR)
- Pattern recognition (MSc ACR)

After coursing the MSc ACR at UPC, the candidate enrolled in the doctorate program Automàtica, Robòtica i Visió at UPC where this thesis proposal has been submitted.

4.2 Task 1: Sensor's uncertainty characterization

The first goal of this thesis is to study the applicability and feasibility of ToF cameras for active sensing purposes and to exhaustively characterize their uncertainty and constraints. The state of the art of the employment of ToF cameras in the field of robotics will be reviewed, paying special attention to those articles based on close range applications. At the same time, and for the sake of characterizing systematic and non-systematic errors on ToF cameras, a full review of the literature will be carried out. That will allow to apply proper depth calibration and correctly parametrize the sensor depending on the task and the scene. But more importantly, it will grant a model of the sensor's uncertainty that will let him apply information-gain approaches.

Since this task has already been fulfilled, a summary of the achieved contributions is presented:

Applicability of ToF cameras in robotics

The distinctive characteristics of ToF cameras have proved to give important advantages in several fields. We can classify the wide range of applications where ToF sensors are used by considering their scenario of application, yielding *scene-related tasks*, *object-related tasks* and *applications involving humans*.

1. **Scene-related tasks**. This kind of applications deal with tasks involving scenes that contain objects like furniture and walls. Observe that the expected range of distances to these objects is relatively wide. A usual framework in these applications is to install the camera on a mobile robot and use it for robot navigation and mapping. One of the areas where ToF sensors are adequate is in obstacle avoidance, because the detection region is not only horizontal (like in laser scanners) but also vertical, allowing to detect obstacles with complex shapes. Clearly, *the most appreciated characteristic of ToF sensors here is the high frame rate*. Some applications also benefit from the metric information obtained with depth images.
2. **Object-related tasks**. ToF cameras have also been successfully used for object and small surface reconstruction, where the range of distances is small. It is expected that some over-saturation problems occur when acquiring depth images. Contrarily, as the range of depths is short, some calibration processes can be simplified. In general the scenario for these applications involves a robotic manipulator or a human-like robot with the task of modeling the object shape.

3. **Applications involving humans**. One of the areas where the use of ToF cameras is most active is in human activity recognition and man-machine interaction. A recent survey on ToF sensors with special attention to 3D graphics and realism has been recently presented [32]. Here, the focus is on technologies appropriate for man-machine interaction. One important characteristic of ToF cameras appreciated in this area is their being a non-invasive technology, contrary to the widely extended use of special gloves, artificial marks, special skin color or special attached devices. ToF camera also offers the advantaged that no special background is needed.

Characterization of ToF cameras

Here, a classification and characterization of the different errors is presented. Depth measurements with ToF cameras face the appearance of both *systematic* and *non-systematic* errors. Generally, systematic errors can be managed by calibration and non-systematic ones by filtering.

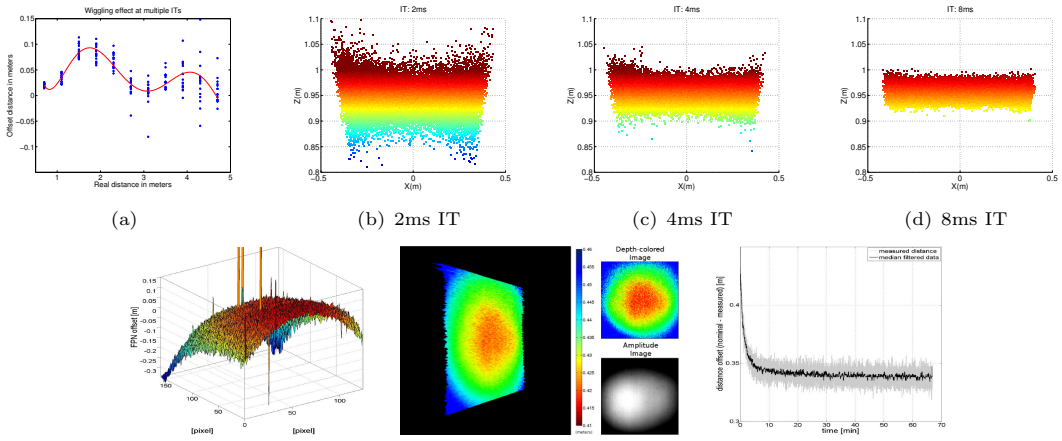

(a) (b) 2ms IT (c) 4ms IT (d) 8ms IT

(e) (f) (g)

Figure 4: Systematic errors. a) Depth distortion offset (Wiggling effect). b-d) Integration-time-related error. e) Built-in pixel-related error. f) Amplitude-related error. g) Temperature-related error (Figure extracted from Kahlmann *et al.* [29]).

Systematic errors

1. *Depth distortion* appears as a consequence of the fact that the emitted infrared light can not be generated in practice as theoretically planned (generally sinusoidal) due to irregularities in the modulation process. This type of error produces an offset that depends only on the measured depth for each pixel. Usually, the error plotted against the distance follows a sinusoidal shape[1] (see Fig. 4(a)). This error is sometimes referred to as *wiggling* or *circular error*.

2. *Integration-time-related error*. Integration time (IT) can be selected by the user. It has been observed that for the same scene different IT cause different depth values in the entire scene (see Fig. 4(b-d)). The main reason for this effect is still a subject of investigation.

[1]This has been explained by means of perturbations on the measured signal phase caused by wrapping of odd harmonics contained in the emitted reference signal [35].

3. *Built-in pixel-related errors* arise from two main sources. On the one hand, errors due to different material properties in CMOS-gates. This produces a constant pixel-related distance offset, leading to different depths measured in two neighbour pixels corresponding to the same real depth. On the other hand, there are latency-related offset errors due to the capacitor charge time delay during the signal correlation process. This can be observed as a rotation of the image plane, i.e. a perpendicular flat surface is viewed with a wrong orientation (see Fig. 4(e)).

4. *Amplitude-related errors* occur due to low or overexposed reflected amplitudes. Depth accuracy is highly related to the amount of incident light. The higher the reflected amplitudes, the higher the depth accuracy. Low amplitude appears more often in the border of the image as the emitted light power is lower than in the center, leading to overestimating depth (see Fig. 4(f)). Contrarily, when the object is too close to the camera or integration time has been chosen too high, saturation can appear and depth measurements will not be valid.

5. *Temperature-related errors* happen because internal camera temperature affects depth processing, explaining why some cameras include an internal fan. Depth values suffer from a drift in the whole image until the temperature of the camera is stabilised (see Fig. 4(g)).

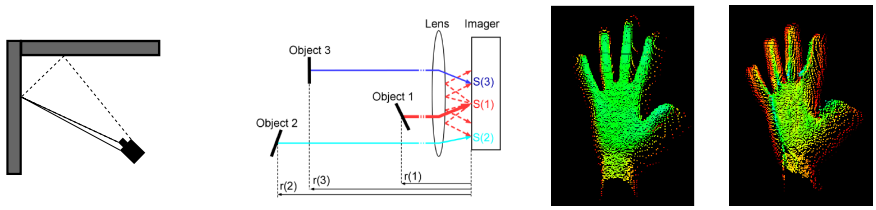

(a) (b) (c) (d)

Figure 5: Non-Systematic errors. a) Multiple light reception. b) Light scattering (Figure extracted from Mure-Dubois, J. and Hügli, H. [41]). c) Static hand. d) Hand moving to the left.

Non-systematic errors

1. *Signal-to-noise ratio* distortion appears in scenes not uniformly illuminated. Low illuminated areas are more susceptible to noise than high illuminated ones. This type of error is highly dependent on the amplitude, the IT parametrisation and the depth uniformity of the scene. Non-uniform depth over the scene can lead to low-amplitude areas (far objects) that will be highly affected by noise.

2. *Multiple light reception* errors appear due to the interference of multiple light reflections captured at each sensor's pixel. These multiple light reflections depend on the low lateral sensor resolution and the geometric shape of the objects in the scene (see Fig. 5(a)).

3. *Light scattering* effect arises due to multiple light reflexions between the camera lens and its sensor (see Fig. 5(b)). This effect produces a depth underestimation over the affected pixels, because of the energy gain produced by its neighbouring pixel reflections [28]. Errors due to light scattering are only relevant when nearby objects are present in the scene. The closer an object, the higher the interference [30].

4. *Motion blurring*, present when traditional cameras are used in dynamic environments, appears also with ToF cameras. This is due to the physical motion of the objects or the camera during the integration time used for sampling (see Fig. 5(c-d)).

Conclusions

This task has contributed to facilitate the evaluation of ToF cameras for robotic purposes and, in the case of being suitable for an application, to easily identify their advantages, drawbacks and constraints [20]. Also, thanks to the ToF camera characterization, a better depth measurement estimation can be achieved by using this information to develop new calibration and filtering algorithms [22].

4.3 Task 2: Modelling under uncertainty

In order to understand a previously unknown *real* scene, a model of it should be build. Taking into account the uncertainty of the sensor's measurements into the 3D data registration process is a key point for correctly build such a model. The use of uncertainty reduction approaches, such as view-based SLAM can dramatically help to improve the 3D registration process if a pre-defined and closed-loop viewpoint trajectory is performed. During this task, efforts will be concentrated on studying and developing a method for propagating the sensor's uncertainty to the sensor's pose through a point cloud registration process and to apply view-based SLAM for improving the 3D model.

This task has already been fulfilled. Therefore, a summary of the achieved contributions is here presented:

3D Modeling under an uncertainty reduction approach

Data fusion for scene or model augmentation has been typically addressed by error minimization methods, such as bundle adjustment [55] or structure from motion [16]. These approaches are often not suitable for real time computation given their iterative nature. Recursive state estimation (e.g., SLAM) is a more suitable choice. The classical EKF-based approach to SLAM for feature-based scene augmentation is also not viable for real time modeling since it requires the computation of fully correlated covariances at each step [18]. The proposal is to use a view-based information-form SLAM method that a) does not maintain a large number of feature estimates, but only a reduced number of pose estimates, and b) is efficiently computed in information form, exploiting the sparsity of such filtering representation [26]. Advantage is taken of the fact that the first and last images in a circular sequence around an object overlap. This allows to impose the loop-closure constraint.

The point cloud registration method used in this approach is based on the well-known ICP algorithm [8, 11, 60], and its variants [40, 47]. The probabilistic data fusion mechanism used in this work requires first order approximations of error propagation. That is, covariance estimates of sensor uncertainty must be propagated through the ICP cost function to compute relative pose covariance estimates between the two generative viewpoints.

The decision of using one cost function or another plays an important role during error propagation, since its derivatives need to be computed. In its simplest form, given a set of matching points from two consecutive point clouds $\mathbf{m}_i = (a, b)$, the ICP cost function takes the form

$$\varepsilon(\mathbf{m}_i, \mathbf{x}_i) = \sum ||\mathbf{x}_i(b) - a||^2. \quad (1)$$

An accurate covariance approximation can be computed using a Monte Carlo simulation, but this is a time-consuming solution and, since speed of execution is really a needed characteristic, finding a closed-form solution is desirable.

Given that the ICP algorithm is basically a cost function minimization procedure, an implicit function between input (point clouds) and the output (the pose) is defined by the minimization process [12]. Albeit the implicit function can not be explicitly known, its Jacobian matrix can be computed. Consequently, the estimated covariance matrix can be computed using the usual first-order approximation of an explicit function

$$\mathbf{\Sigma}_i = \nabla \mathbf{f}\, \mathbf{\Sigma}_s\, \nabla \mathbf{f}^{\mathrm{T}}, \tag{2}$$

where $\nabla \mathbf{f}$ is the explicit function's Jacobian matrix, $\mathbf{\Sigma}_s$ the sensor covariance matrix and $\mathbf{\Sigma}_i$ the computed relative pose covariance matrix.

The Jacobian matrix of the ICP implicit function can be computed by means of the implicit function theorem. In our case, for an unconstrained minimization problem, the Jacobian matrix becomes

$$\nabla \mathbf{f} = \left(\frac{\partial^2 \varepsilon}{\partial \mathbf{x}_i^2} \right)^{-1} \frac{\partial^2 \varepsilon}{\partial \mathbf{m}_i\, \partial \mathbf{x}_i}. \tag{3}$$

Since the approach uses the point to point Euclidean distance error as a cost function in the registration process, the application of the implicit function theorem is straightforward. It is important to notice however that this type of approximation propagates the error from sensor measurements to the sensor's relative pose. Therefore, the parametrization of the cost function will have to include the real sensor measurements as its only input variables. For instance, if a point-to-plane ICP algorithm is used, its point-to-plane function will have to be accommodated into the implicit function and derived consequently. It is not correct to pre-compute the virtual point of the plane correspondence and then apply a point-to-point cost function.

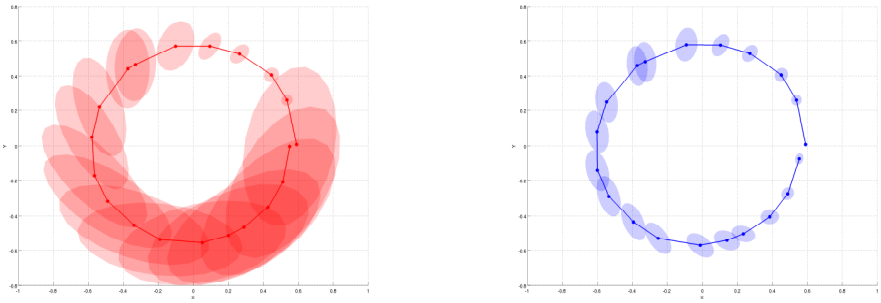

(a) Robot trajectory after all ICP results are aggregated

(b) Revised robot trajectory after the loop is closed with the view-based SLAM method

Figure 6: Robot pose trajectory. Frame a) shows the calculated trajectory and uncertainty estimates after all ICP results are aggregated, but before the loop is closed. Each pose accumulates the estimated error from the previous pose. Frame b) once the loop is closed, uncertainty is reduced and the complete trajectory is corrected.

Conclusions

As a contribution, this task has achieved to improve 3D object modelling by propagating sensor's uncertainty through a point cloud registration process. Iterative point cloud registration

algorithms, such as Iterative Closest Point (ICP), smoothly refine previous coarse registration without taking into account the measurement uncertainty. This new approach significantly improves the overall 3D model once a loop-closure is achieved [19].

Fig. 6 shows the estimated robot trajectories for the cases of ICP relative pose aggregation, and SLAM-based loop closure. After closing the loop, the final trajectory (blue) is closer to a circular shape than not the one achieved purely from accumulating ICP motion estimates (red). The red trajectory tends to describe the typical spiral shape characteristic from error accumulation.

4.4 Task 3: Active sensing for 3D modelling of rigid objects

This task contains both tasks 3 and 4 from Section 2.1. Pre-defined trajectories constrain task's versatility. Since the goal is to actively plan our next vantage point based on the current state of the data interpretation and the goal of the task, a more dynamic system should be implemented. Therefore, it is necessary to find a task-based criterion for generating multiple vantage points so they can wisely be evaluated by an information-gain decision-making algorithm. For instance, a perfect match for 3D object modelling tasks is a combination of a shape-based viewpoint planner and a viewpoint information-gain-based evaluation. During the development of this task, a stay at the German Aerospace Center (DLR) has been carried out under the supervision of Michael Suppa and Stefan Fuchs where the studies have been focused on:

Task 3.1 Reviewing the current active sensing techniques for 3D object modelling (Next-Best-View algorithms). Special attention will be paid to:

1. Shape-based viewpoint planning techniques.
2. Information-gain-based evaluation methods.

Task 3.2 Combining shape-based viewpoint planning techniques with information-gain-based evaluation for optimal 3D object modelling.

Task 3.3 Learning and applying depth calibration and filtering techniques over ToF cameras measurements.

Since this task has already been fulfilled, a summary of the achieved contributions is here presented:

Shape-based viewpoint planner

In order to determine a new vantage point accordingly to the information gain, a search space consisting of multiple viewpoints (possible sensor positions and orientations) is required as input. Since the workspace around an object features an infinite number of views, many authors reduce the search space by sampling candidate views around an approximate sphere or cylinder [7, 43, 56]. Their candidate views always point to the center of their figures and, consequently, the sensor can not be positioned in a way that achieves optimal modeling results.

In this work, the *Viewpoint Estimator* [34] algorithm is used. This algorithm generates viewpoints by detecting boundary trends in a triangular mesh. It works as follows. Once new 3D data are acquired, a triangular mesh is reconstructed in a real-time stream as suggested by [9]. A quadratic patch is then fitted to each boundary region and new viewpoints, perpendicular to those patches, are then generated. Therefore, the search space is not limited to a set of pre-defined poses over a sphere or cylinder but it allows for any position and orientation. Depending on their position, relative to the sensor, the detected boundaries are classified as left, right, top

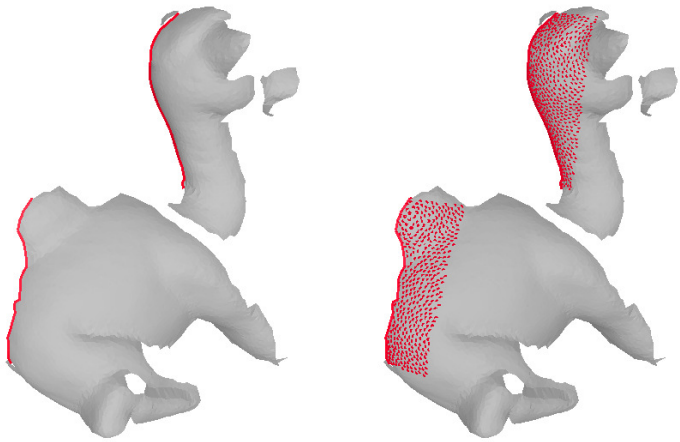

(a) Boundary classification (b) Quadratic patch fitting

Figure 7: Example of two boundaries obtained from a partial camel mesh, which are classified as left boundaries. A region growing is performed in order to fit a quadratic patch.

and bottom. In their work, the next viewpoint was chosen heuristically by first going through the left, then right, top and bottom boundaries. Figure 7 shows an example of two boundaries classified as left and the subsequent region growing, which is used to fit a quadratic patch.

Information-gain-based evaluation method

In Information Theory, *information gain* is a probabilistic measure of how significant a new state estimate of the environment is. The concept of information gain is equivalent to the one of uncertainty or entropy reduction. Entropy, as defined by [51], is computed as:

$$H(x) = -\sum_{X} p(x) \log p(x), \tag{4}$$

where X is a finite set of values of a discrete random variable x that has $p(x)$ as probability distribution function. For a n multivariate Gaussian distribution with covariance matrix Σ, entropy can be computed as:

$$H(x) = \frac{1}{2} \log((2\pi)^n |\Sigma|). \tag{5}$$

As [52] already pointed out, using the determinant over all possible measurements for computing the information gain is computationally expensive. Based on his work, our approach uses the trace of the covariance matrix instead of its determinant and, therefore, efficiently computes the overall gain. This is possible thanks to having the same representation units for all the observable features and, consequently, avoiding scalability problems. Finally, and despising the constants, the entropy of a discrete random variable can be efficiently computed as:

$$H(x) = \sum_{i=0}^{3n} \log(\Sigma_{ii}). \tag{6}$$

Scene Representation: 3D Occupancy Grid

A 3D occupancy grid is a map of a 3D space represented by a set of random variables, which are uniformly distributed on a discrete grid. These random variables are binary and specify whether each of the grid cells is occupied or free. Usually occupancy grid maps are used for building a consistent map after solving the SLAM problem, since they assume exact robot's pose information [54]. In a different way, our approach does not use the occupancy grid map as a final result but as a tool to evaluate the information gain of multiple possible view poses.

Our 3D occupancy grid map is based on a probabilistic voxel space defined by a multiresolution octree structure. All 3D grid cells, also called voxels, have associated a covariance matrix depending on all the history of measurements. At the same time, each voxel is defined by three possible occupancy types: *occupied*, *free* or *unknown*. By using the covariance matrix as an uncertainty voxel-related measurement, our approach can optimally obtain the information gain taking into account the orientation of the sensor. This is an important feature when using a noisy sensor such as a ToF camera, since the error is usually bigger on one component.

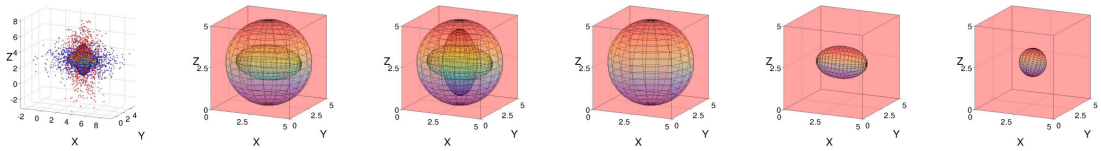

(a) (b) (c) (d) (e) (f)

Figure 8: Graphical interpretation through ellipsoids of the covariance reduction inside a voxel. Figure a) shows two independent simulated readings of a point in space, which are taken to be perpendicular for clarity. Figure d) shows the a priori uncertainty of an unknown voxel represented as a covariance matrix and visualized as a sphere inscribed inside the voxel cube. Pairs of figures (b-e) and (c-f) show how the covariance of a voxel gets updated after combining one or both readings, respectively.

Expected Gain Using an Occupancy Grid

Initially, all voxel states are set to *unknown*, state with the highest uncertainty. Once new sensor data are obtained, the states of all voxels intersected by a ray are updated. Depending on whether a voxel is crossed by a ray-trace or whether it encloses a new measurement, the voxel state is set to *free* or to *occupied*, respectively. Also, each *occupied* voxel is assigned its measurement covariance matrix $\mathbf{\Sigma}_i$ in order to posteriorly compute the information gain of new viewpoints. If the voxel was previously defined *occupied*, both the new covariance and the former are combined as shown in Fig. 8 by

$$(\Sigma_i)^{-1} = (\Sigma_i^{t-1})^{-1} + (\Sigma_i^t)^{-1}. \tag{7}$$

Only voxels with *unknown* and *occupied* states would be considered for estimating the information gain, since *free* voxels do not provide any information. The reason for this behaviour is to minimize the effect of non-filtered noise and possible miss-readings due to non-systematic ToF camera errors. Once the viewpoint estimator recommends a set of $\boldsymbol{n}$ viewpoints, their expected information gain ($\boldsymbol{IG}$) is computed. Every viewpoint is simulated by ray-tracing from the sensor's pose to the occupancy grid. Each colliding ray updates the corresponding voxel's

covariance matrix and a copy is kept in memory as a sparse matrix

$$\boldsymbol{A} = \begin{pmatrix} \boldsymbol{\Sigma}_0 & 0 & \cdots & 0 \\ 0 & \boldsymbol{\Sigma}_1 & \ddots & \vdots \\ \vdots & \ddots & \ddots & 0 \\ 0 & \cdots & 0 & \boldsymbol{\Sigma}_n \end{pmatrix}. \tag{8}$$

Finally, the overal expected information gain is computed as

$$\boldsymbol{IG} = \sum_{i=0}^{3n} \log(\boldsymbol{A_{ii}}), \tag{9}$$

Conclusions

The achievement of this task has contributed to extend information-gain decision-making as a task-based criterion for active sensing [23]. Active view planning is viewed as a space characterization task whose goal is to answer the question: where should the sensor be placed for locating specific characteristics? Because it involves spatial characteristics (or at least located in space), the proposed approach uses a voxelized space where each voxel contains a complete 3×3 covariance. This representation allows to account not only for exploration (unknown areas) but also for refinement, that is, the information gain of seeing characteristics again from a different point of view.

4.5 Task 4: Vantage point for disambiguation purposes

Once shape-based viewpoint planning techniques have been satisfactorily tested for raw 3D data exploration purposes (modelling), higher level features can be abstracted from the scene, and consequently more complex tasks can be achieved. For instance, an incremental step towards active sensing would be the computation of a vantage point for disambiguation purposes. Ambiguity into a scene appears when, after feature model fitting evaluation, low confident values are returned or also when specific 3D features are detected. Vantage point planning strategies are then necessary to add new information into the system and therefore clarify its perception.
This task can be divided in two sub-tasks:

Task 4.1 Improve scene segmentation by combining color/intensity images with model-based fitting and depth data.

Task 4.2 Review of 3D feature extraction algorithms. If needed, develop new features for specific plant structure disambiguation purposes.

This is the last completed task, and these are the achieved contributions:

Scene segmentation

Here it is presented a novel algorithm for the segmentation of dense color images into surface patches using sparse depth data, acquired using either ToF or stereo techniques. The color images are segmented at different resolutions, 3D surfaces are then fitted to the color-segment areas using sparse depth data, and a new segmentation is found by minimizing the total fitting error while giving preference to segments at lower resolutions. The method has been demonstrated to segment a variety of images of domestic objects and plants into their composite surfaces and

shown to be applicable to different kinds of depth information, i.e., ToF and stereo. The method showed robust results for the given parameter set and also was demonstrated to work well for images of plants that contain many depth layers, occlusions, and leaf boundaries of weak contrast.

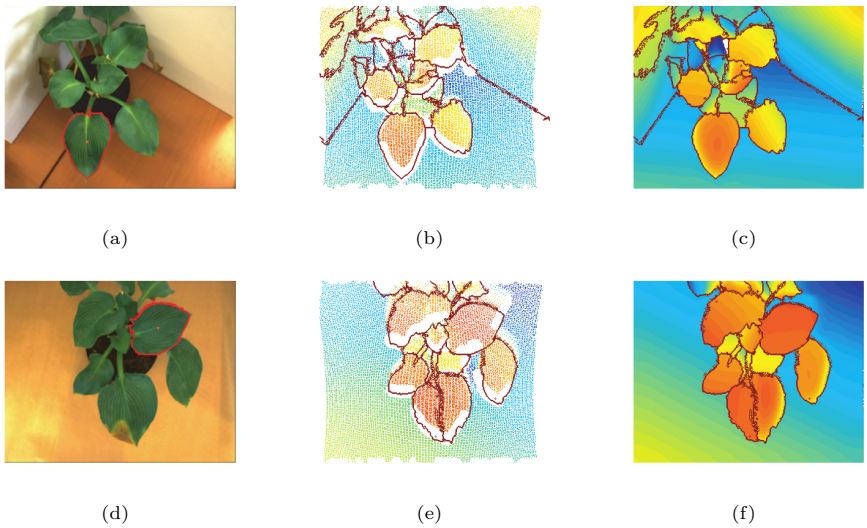

(a) (b) (c)

(d) (e) (f)

Figure 9: Segmentation results for plants. (a-d): Original color image together with an exemplary candidate segment boundary (marked in red) (see text). (b-e): Initial ToF sparse depth plotted together with final segment boundaries. (c-f): Fitted depth using segment surface models plotted together with the final segment boundaries.

Plant images are challenging because they contain many depth layers and occlusions, caused by overlapping leaves, and weak contrast boundaries separating adjacent leaves. The results are presented in Fig. 9. In the left panels, the original color images are shown. In the middle panels, final segment boundaries (after region growing) are presented together with the initial depth data. In the right panels, the final fitted depths are shown together with the final segment boundaries. Even though plants exhibit complicated shapes and have many occlusions, most of the main surfaces have been found, often corresponding to leaves or at least part of leaves, and curved shapes could be modelled correctly in most cases (for example the large leaf at the bottom in Fig. 9(a)). Basic segment properties such as mean color, size, and mean fitting error are computed, and, based on these criteria, candidate segments (e.g. for robot manipulation) are selected representing leaf structures. An exemplary candidate segment has been marked red for each plant (Fig. 9, left panels). Also the center point of the segments has been marked red.

Features for disambiguation

Here, a novel method to efficiently estimate a new vantage point for improving plant monitoring is presented. The method takes advantage of jump-edge flying points, typical erroneous data from a ToF camera, for finding a suitable solution to two common monitoring tasks, getting a better view of an occluded target leaf and resolving ambiguity in the number of leaves. The method can be executed in real-time since it does not use any cost function minimization approach or any complex leaf model fitting but a geometrical approach and a simple planar leaf model.

Jump-edge measurements are a consequence of false measurements and therefore generally filtered from the data sets [24, 28, 31], even the new Kinect sensor filters internally these type of

misreadings. But, for the proposed monitoring tasks, the appearance of these false measurements are indicative of possible model misinterpretation or object occlusion. Figure 10(a) shows a schematic representation of how such a vantage point is computed.

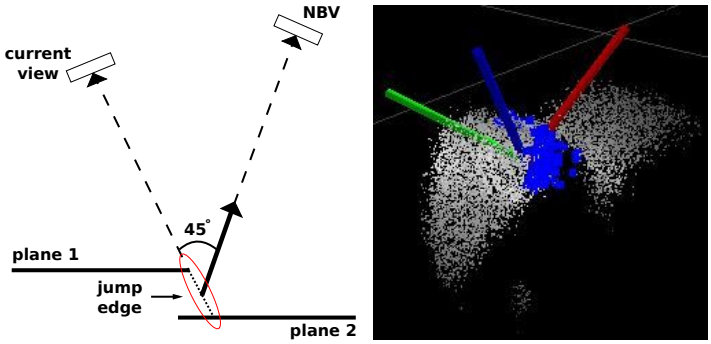

(a) 2D new vantage point schematic representation

(b) Jump-edge points (Blue)

Figure 10: False depth measurements (jump-edge points) detection helps to compute the next viewpoint to uncover occluded leaves and to disambiguate the number of observed leaves. Figure (a) shows the 2D schematic representation of the algorithm. Figure (b) shows, in blue, the 3D jump-edge points.

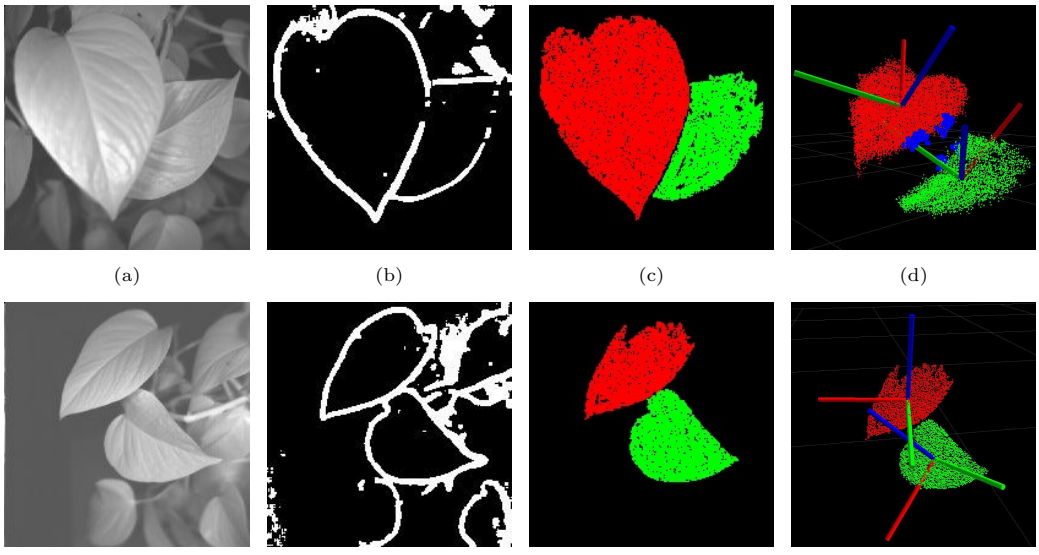

(a) (b) (c) (d)

(e) (f) (g) (h)

Figure 11: Scene containing a detected leaf occlusion. Top row shows the scene before applying the vantage point algorithm, images (a-d). Bottom row shows the scene observed from the new viewpoint, images (e-h).

Figure 11 shows the resulting data of a scene where an occlusion of a leaf is clearly identified. By executing the jump-edge filter over the 3D data, the countours of each leaf are extracted (Fig. 11(b)). At the same time, the plane segmentation process provides the estimation of the

different planes (Fig. 11(c)). Figure 11(d) shows, in a 3D rotated view, the extracted jump-edge points that fall just in the frontier between both leaves. These points are the ones that allow us to compute the vantage point whose result is displayed at the bottom row of Fig. 11. By comparing the image pairs Fig. 11(a, e) and Fig. 11(c, g), it can be seen by moving the camera to the computed vantage point the overall perception of the occluded leaf surface is significally improved.

Conclusions

The completion of this task has contributed to develop novel algorithms for leaf segmentation and task-related 3D feature extraction for initial active sensing purposes [21]. The identification of the different parts of a plant and the detection of significant spatial features will provide the necessary clues for solving higher complexity active sensing tasks.

4.6 Task 5: Task-oriented active sensing of complex objects (plants)

This task is dedicated to build a unified framework for complex task-oriented active sensing driven by a 3D-space-based information-gain goal. This research aims to define a set of exploratory complex tasks over plants that profit from this approach. Tasks will be such as: what is the overall occupied space of a plant, what is its topology or which is the best leaf for probing on the plant. During this stage the studies will also focus on how to extend the use of ToF cameras under different illumination situations in order to cover as many as possible plant's location, such as outdoor (where sun light distorts the readings) or indoor (where light is under control).

Task 5.1 Detect external illumination and control camera parameters for depth acquisition improvement.

Task 5.2 Unify the task-oriented active sensing approach.

1. Describe and characterize exploratory tasks over plants.
2. Build task-related cost functions to partially pre-model the scene.

Expected contributions

At the end of the execution of this task, it is expected to have finished all the experimental work and to have developed a unified framework for task-oriented active sensing based on 3D-space-based information-gain.

Task 6: Compilation of results

Task 6 is assigned to the final duty of gathering together the experimental data and analysing the overall results in order to let the author write down and submit his PhD thesis.

Figure 12 presents the schedule for the tasks described through Sections 4.1 to 4.6 in a Gantt chart that spans over three years, in this, T stands for a three months period, so that *T1* represents the first three months of a year. The tasks already attained are shown with crosshatch points.

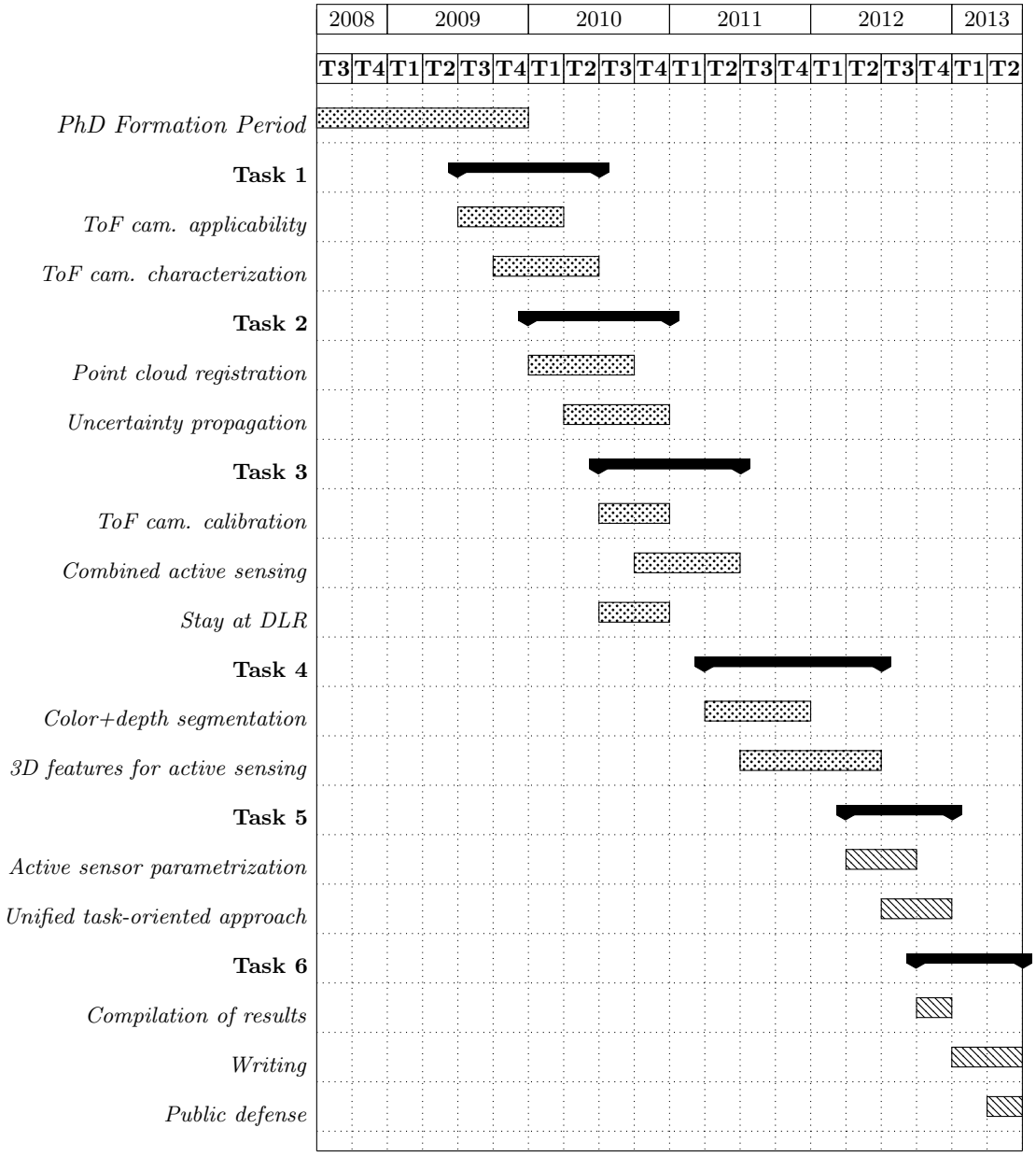

Figure 12: Workplan of the proposed thesis

5 Resources

Except for a 6 months stay at the German Aerospace Center (DLR), all the work has been and will be developed under the framework of the Perception and Manipulation sub-line at the *Institut de Robòtica i Informàtica Industrial (UPC-CSIC)* from Barcelona. Funding has been obtained from several projects at European, National and Regional level, such as: PACOPLUS (IST-FP6-

IP-027657), PAU (DPI2008-06022), GARNICS (FP7-247947), SGR ROBÒTICA (2009SGR155) and PAU+(DPI2011-27510). The author is financed by a JAEPredoc grant provided by the Spanish Council of Scientific Research (CSIC).

6 Publications

In this section, the reader can find the complete list of accepted and submitted publications since the beginning of the PhD:

Journals

1. S. Foix, S. Kriegel, S. Fuchs, G. Alenyà and C. Torras. "*Explicit modelling of ToF camera uncertainty to improve complex 3D shape acquisition*", submitted to a journal.
2. G. Alenyà, B.Dellen, S. Foix and C. Torras. "*Leaf segmentation from ToF data for robotized plant probing*," IEEE Robotics and Automation Magazine, to appear in 2012.
3. S. Foix, G. Alenyà and C. Torras. "*Lock-in time-of-flight (ToF) cameras: a survey*," IEEE Sensors Journal, 11(9): 1917-1926, 2011.

Conferences and workshops

1. W. Kizma, S. Foix and G. Alenyà. "*Plant leaf analysis using Time of Flight camera under sun, shadow and room conditions*," Paper submitted, 2012.
2. S. Foix, S. Kriegel, S. Fuchs, G. Alenyà and C. Torras. "*Information-gain view planning for free-fom object reconstruction with a 3D ToF camera*," International Conference on Advanced Concepts for Intelligent Vision Systems, 2012.
3. B. Dellen, G. Alenyà, S. Foix and C. Torras. "*Segmenting ToF data into surface patches for robotized leaf probing*," accepted at IEEE IROS Workshop on agricultural robotics, 2012, Algarve, Portugal.
4. S. Foix, G. Alenyà and C. Torras. "*Towards plant monitoring through next best view*," 14th International Conference of the Catalan Association for Artificial Intelligence, 2011, Lleida, in Artificial Intelligence Research and Development, Vol 232 of Frontiers in Artificial Intelligence and Applications, pp. 101-109, IOS Press.
5. B. Dellen, G. Alenyà, S. Foix and C. Torras. "*Segmenting color images into surface patches by exploiting sparse depth data*," IEEE Workshop on Applications of Computer Vision, 2011, Kona, Hawaii, pp. 591-598.
6. S. Foix, G. Alenyà, J. Andrade-Cetto and C. Torras. "*Object modelling using a ToF camera under an uncertainty reduction approach*," IEEE International Conference on Robotics and Automation, 2010, Anchorage, pp. 1306-1312.
7. B. Dellen, G. Alenyà, S. Foix and C. Torras. "*3D object reconstruction from Swissranger sensor data using a spring-mass model*," 4th International Conference on Computer Vision Theory and Applications, 2009, Lisboa, pp. 368-372, 2009, INSTICC Press.

Technical reports

1. S. Foix, G. Alenyà and C. Torras. "*Exploitation of time-of-flight (ToF) cameras*," Technical Report IRI-TR-10-07, Institut de Robòtica i Informàtica Industrial, CSIC-UPC, 2010.

7 Bibliography

[1] 3D vision sensors, http://www.ifm.com. Ifm electronic gmbh, 2009.

[2] SR-Cameras, http://www.mesa-imaging.ch. MESA Imaging AG, 2009.

[3] PMD-Cameras, http://www.pmdtec.com. PMDTechnologies GmbH, 2009.

[4] G. Alenyà, B. Dellen, and C. Torras. 3d modelling of leaves from color and tof data for robotized plant measuring. In *Proc. IEEE Int. Conf. Robot. Automat.*, pages 3408–3414, Shanghai, May 2011.

[5] T. Arbel and F. P. Ferrie. On the sequential accumulation of evidence. *Int. J. Comput. Vision*, 43(3):205–230, 2001. doi: 10.1023/A:1011187530616.

[6] R Bajcsy. Active perception. *Proc. IEEE*, 76:966–1005, 1988.

[7] J. E. Banta, L. M. Wong, C. Dumont, and M. A. Abidi. A next-best-view system for autonomous 3-D object reconstruction. *IEEE Trans. Syst., Man, Cybern. A*, 30(5):589–598, Sep. 2000.

[8] P.J. Besl and N.D. McKay. A method for registration of 3D shapes. *IEEE Trans. Pattern Anal. Machine Intell.*, 14(2):239–256, Feb. 1992.

[9] Tim Bodenmüller. *Streaming surface reconstruction from real time 3D measurements*. PhD thesis, Technische Universität München (TUM), 2009.

[10] S. Chen, Y. Li, J. Zhang, and W. Wang. *Active sensor planning for multiview vision tasks*. Springer-Verlag, Berlin Heidelberg, 2008.

[11] Y. Chen and G. Medioni. Object modeling by registration os multiples ranges images. In *Proc. IEEE Int. Conf. Robot. Automat.*, volume 3, pages 2724–2729, Sacramento, Apr. 1991.

[12] J.C. Clarke. Modelling uncertainty: A primer. Technical Report 2161/98, University of Oxford. Dept. Engineering science, 1998.

[13] C. I. Connolly. The determination of next best views. In *Proc. IEEE Int. Conf. Robot. Automat.*, volume 2, pages 432–435, St. Louis, Mar. 1985.

[14] B. Curless and M. Levoy. A volumetric method for building complex models from range images. In *Computer Graphics. Proc. ACM SIGGRAPH Conf.*, pages 303–312, New York, Aug. 1996. ACM Press.

[15] F. Deinzer, C. Derichs, and H. Niemann. A framework for actively selecting viewpoints in object recognition. *Int. J. Pattern Recogn. Artif. Intell.*, 23(4):765–799, 2009.

[16] F. Dellaert, S.M. Seitz, C.E. Thorpe, and S. Thrun. Structure from motion without correspondence. In *Proc. 14th IEEE Conf. Comput. Vision Pattern Recog.*, volume 2, pages 557–564, Hilton Head, SC, Jun. 2000.

[17] J. Denzler and C.M. Brown. Information theoretic sensor data selection for active object recognition and state estimation. *IEEE Trans. Pattern Anal. Machine Intell.*, 24(2):145–157, 2002. doi: 10.1109/34.982896.

[18] M. W. M. G. Dissanayake, P. Newman, S. Clark, H. F. Durrant-Whyte, and M. Csorba. A solution to the simultaneous localization and map building (SLAM) problem. *IEEE Trans. Robot. Automat.*, 17(3):229–241, Jun. 2001.

[19] S. Foix, G. Alenyà, J. Andrade-Cetto, and C. Torras. Object modeling using a ToF camera under an uncertainty reduction approach. In *Proc. IEEE Int. Conf. Robot. Automat.*, pages 1306–1312, Anchorage, May 2010.

[20] S. Foix, G. Alenyà, and C. Torras. Exploitation of Time-of-Flight (ToF) cameras. Technical Report IRI-DT-10-07, IRI, UPC, 2010.

[21] S. Foix, G. Alenyà, and C. Torras. Towards plant monitoring through next best view. In *Proc. 14th Int. Conf. Cat. Assoc. Artificial Intelligence*, Lleida, Oct. 2011.

[22] S. Foix, G. Alenyà, and C. Torras. Lock-in Time-of-Flight (ToF) cameras: a survey. *IEEE Sensors J.*, 11(9):1917–1926, Sep. 2011.

[23] S. Foix, S. Kriegel, S. Fuchs, G. Alenyà, and C. Torras. Information-gain view planning for free-form object reconstruction with a 3D ToF camera. In *Internatial Conference on Advanced Concepts for Intelligent Vision Systems*, Sep. 2012.

[24] S. Fuchs and S. May. Calibration and registration for precise surface reconstruction with time of flight cameras. *Int. J. Int. Syst. Tech. App.*, 5(3-4):274–284, 2008. ISSN 1740-8865. doi: http://dx.doi.org/10.1504/IJISTA.2008.021290.

[25] S.B. Gokturk, H. Yalcin, and C. Bamji. A time-of-flight depth sensor - system description, issues and solutions. In *Proc. IEEE CVPR Workshops*, pages 35–35, Washington, D. C., June 2004. doi: 10.1109/CVPR.2004.17.

[26] V. Ila, J. M. Porta, and J. Andrade-Cetto. Information-based compact Pose SLAM. *IEEE Trans. Robot.*, 26(1):78–93, Feb. 2010.

[27] Z. Jia, Y. Chang, and T Chen. A general boosting-based framework for active object recognition. In *Proc. British Machine Vision Conf.*, pages 46.1–46.11. BMVA Press, Sep. 2010. doi: 10.5244/C.24.46.

[28] T. Kahlmann and H. Ingensand. Calibration and development for increased accuracy of 3D range imaging cameras. *J. Appl. Geodesy*, 2(1):1–11, 2008. doi: 10.1515/JAG.2008.001.

[29] T. Kahlmann, F. Remondino, and H. Ingensand. Calibration for increased accuracy of the range imaging camera Swissranger^{TM}. In *ISPRS Commission V Symposium*, pages 136–141, Dresden, Sep. 2006.

[30] W. Karel. Integrated range camera calibration using image sequences from hand-held operation. In *Proc. ISPRS Conf.*, volume 37, pages 945–952, Beijing, Jul. 2008.

[31] W. Karel, P. Dorninger, and N. Pfeifer. In situ determination of range camera quality parameters by segmentation. In *Proc. 8th Int. Conf. on Opt. 3D Meas. Tech.*, pages 109 – 116, Zurich, July 2007.

[32] A. Kolb, E. Barth, R. Koch, and R. Larsen. Time-of-flight sensors in computer graphics. In *Eurographics (State-of-the-Art Report)*, pages 119–134, 2009.

[33] Björn Krebs, M. Burkhardt, and Bernd Korn. Handling uncertainty in 3d object recognition using bayesian networks. In H. Burkhardt and B. Neumann, editors, *Proc. 5th European Conf. Comput. Vision*, volume 2 of *Lect. Notes Comput. Sci.*, pages 782–795, Freiburg, Jun. 1998.

[34] S. Kriegel, T. Bodenmüller, M. Suppa, and G. Hirzinger. A surface-based next-best-view approach for automated 3D model completion of unknown objects. In *Proc. IEEE Int. Conf. Robot. Automat.*, pages 4869–4874, Shanghai, May 2011.

[35] R. Lange. *3D time-of-flight distance measurement with custom solid-state image sensors in CMOS/CCD-technoloty*. PhD thesis, Univ. Siegen, Germany, 2000.

[36] C.B. Madsen and H.I. Christensen. A viewpoint planning strategy for determining true angles on polyhedral objects by camera alignment. *IEEE Trans. Pattern Anal. Machine Intell.*, 19(2):158 –163, Feb. 1997. doi: 10.1109/34.574798.

[37] N. Massios and R. Fisher. A best next view selection algorithm incorporating a quality criterion. In J. N. Carter and M. S. Nixon, editors, *Proc. British Machine Vision Conf.*, pages 780 – 789, Southampton, 1998.

[38] J. Maver and R. Bajcsy. Occlusions as a guide for planning the next view. *IEEE Trans. Pattern Anal. Machine Intell.*, 15(5):417–433, May 1993.

[39] S. May, D. Droeschel, D. Holz, S. Fuchs, E. Malis, A. Nuchter, and J. Hertzberg. Three-dimensional mapping with time-of-flight cameras. *J. Field Robotics*, 26(11-12):934–965, Nov.-Dec. 2009. doi: 10.1002/rob.20321.

[40] J. Minguez, L. Montesano, and F. Lamiraux. Metric-based iterative closest point scan matching for sensor displacement estimation. *IEEE Trans. Robot.*, 22(5):1047–1054, Oct. 2006.

[41] J. Mure-Dubois and H. Hügli. Real-time scattering compensation for time-of-flight camera. In *Proc. 5th Int. Conf. Comput. Vision Systems*, Bielefeld, March 2007. doi: 10.2390/biecoll-icvs2007-167.

[42] D. Papadopoulos-Orfanos and F. Schmitt. Automatic 3-d digitization using a laser rangefinder with a small field of view. In *Proc. Int. Conf. Recent Advances in 3D Digital Imag. and Model.*, Otawa, May 1997.

[43] R. Pito. A solution to the next best view problem for automated surface acquisition. *IEEE Trans. Pattern Anal. Machine Intell.*, 21(10):1016–1030, Oct. 1999. ISSN 0162-8828. doi: 10.1109/34.799908.

[44] M.K. Reed and P.K. Allen. A robotic system for 3d model acquisition from multiple range images. In *Proc. IEEE Int. Conf. Robot. Automat.*, pages 2509 – 2514, Albuquerque, Apr. 1997.

[45] S. Dutta Roy, S. Chaudhury, and S. Banerjee. Active recognition through next view planning: A survey. *Pattern Recogn.*, 37(3):429–446, 2004.

[46] S.D. Roy, S. Chaudhury, and S. Banerjee. Recognizing large 3-d objects through next view planning using an uncalibrated camera. In *Proc. IEEE Int. Conf. Comput. Vision*, volume 2, pages 276–281, Vancouver, Canada, Jul. 2001. doi: 10.1109/ICCV.2001.937636.

[47] S. Rusinkiewicz and M. Levoy. Efficient variants of the ICP algorithm. In *Proc. 3rd Int. Conf. 3D Digital Imaging Modeling*, pages 145–152, Quebec, May 2001.

[48] A. Saxena, L. Wong, and A. Y. Ng. Learning grasp strategies with partial shape information. In *Proc. 23th AAAI Conf. on Artificial Intelligence*, pages 1491–1494, Chicago, Jul. 2008.

[49] B. Schiele and J.L. Crowley. Transinformation for active object recognition. In *Proc. IEEE Int. Conf. Comput. Vision*, pages 249 –254, Bombay, Jan. 1998.

[50] W. R. Scott and G. Roth. View planning for automated three-dimensional object reconstruction and inspection. *ACM Computing Surveys*, 35(1):64–96, Mar. 2003.

[51] C. E. Shannon. A mathematical theory of communication. *Bell Syst. Tech. J.*, 27:379–423, 1948.

[52] R. Sim. Stable exploration for bearings-only SLAM. In *Proc. IEEE Int. Conf. Robot. Automat.*, pages 2422–2427, Barcelona, Apr. 2005.

[53] G. Tarbox and S. Gottschlich. Planning for complete sensor coverage in inspection. *Comput. Vis. Image Und.*, 61(1):84 – 111, Jan. 1995.

[54] S. Thrun, W. Burgard, and D. Fox. *Probabilistic Robotics*. MIT Press, Cambridge, 2005.

[55] B. Triggs, P.F. McLauchlan, R.I. Hartley, and A.W.Fitzgibbon. Bundle adjustment - A modern synthesis. In *Proc. Int. Workshop on Vision Algorithms*, volume 1883 of *Lect. Notes Comput. Sci.*, pages 153–177, Corfu, Sep. 1999.

[56] J. I. Vásquez-Gómez, E. López-Damian, and L. E. Sucar. View planning for 3D object reconstruction. In *Proc. IEEE/RSJ Int. Conf. Intell. Robots Syst.*, pages 4015–4020, St. Louis, USA, Oct. 2009.

[57] P. Whaite and F. P. Ferrie. Autonomous exploration: Driven by uncertainty. *IEEE Trans. Pattern Anal. Machine Intell.*, 19(3):193–205, Mar. 1997.

[58] Z. Xu, R. Schwarte, H. Heinol, B. Buxbaum, and T. Ringbeck. Smart pixel - photonic mixer device (PMD) / New System Concept of a 3D-imaging-on-a-chip. In *Proc. 5th Int. Conf. Mechatronics and Machine Vision in Practice*, pages 259–264, Nanjing, Sep. 1998.

[59] X. Yuan. A mechanism of automatic 3D object modeling. *IEEE Trans. Pattern Anal. Machine Intell.*, 17(3):307–311, Mar. 1995. doi: 10.1109/34.368196.

[60] Z. Zhang. Iterative point matching for registration of free-form curves and surfaces. *Int. J. Comput. Vision*, 13:119–152, 1994.